

PI(3,4,5)P₃ and PI(4,5)P₂ Lipids Target Proteins with Polybasic Clusters to the Plasma Membrane

Won Do Heo,¹ Takanari Inoue,¹ Wei Sun Park,¹ Man Lyang Kim,¹ Byung Ouk Park,² Thomas J. Wandless,¹ Tobias Meyer^{1*}

Many signaling, cytoskeletal, and transport proteins have to be localized to the plasma membrane (PM) in order to carry out their function. We surveyed PM-targeting mechanisms by imaging the subcellular localization of 125 fluorescent protein–conjugated Ras, Rab, Arf, and Rho proteins. Out of 48 proteins that were PM-localized, 37 contained clusters of positively charged amino acids. To test whether these polybasic clusters bind negatively charged phosphatidylinositol 4,5-bisphosphate [PI(4,5)P₂] lipids, we developed a chemical phosphatase activation method to deplete PM PI(4,5)P₂. Unexpectedly, proteins with polybasic clusters dissociated from the PM only when both PI(4,5)P₂ and phosphatidylinositol 3,4,5-trisphosphate [PI(3,4,5)P₃] were depleted, arguing that both lipid second messengers jointly regulate PM targeting.

Small guanine triphosphatases (GTPases) from the Ras, Rho, Arf, and Rab subfamilies often exert their role at the PM where they control diverse signaling, cytoskeletal, and transport processes (1–3). KRas, CDC42, and other family members require a cluster of positively charged amino acids for PM localization and activity (2, 4). In vitro studies indicate that the physiological PM binding partner of such polybasic clusters could be phosphatidylserine, which has one negative charge, or the less abundant lipid second messenger PI(4,5)P₂, which has four negative charges (5–7). We took a genomic survey approach and investigated PM-targeting mechanisms by confocal imaging of 125 cyan fluorescent protein (CFP)–tagged constitutively active small GTPases (8). Expression in NIH3T3 and HeLa cells showed that 48 small GTPases were fully or partially localized to the PM (Fig. 1A and fig. S1).

Thirty-seven of these PM-localized small GTPases had C-terminal polybasic clusters consisting of four or more Lys or Arg residues at positions 5 to 20 from the C terminus (Fig. 1B and fig. S1). Polybasic clusters were found in three forms: they were present together with N-terminal myristoylation consensus sequences (as in Arl4) (9) or with C-terminal prenylation consensus sequences (as in KRas) (5, 6, 10), or they lacked lipid modifications (as in Rit) (11). We called these three combinations polybasic-myristoyl, polybasic-prenyl, and polybasic-nonlipid PM-targeting motifs, respectively. A number of remaining PM-targeted small GTPases had a combined prenylation and palmitoylation consensus sequence that mediated PM targeting

without requiring polybasic amino acids (as does that of HRas) (Fig. 1, A and C) (5, 12). Arf6 lacked a specific targeting motif and was only localized to the PM in its guanine triphosphate (GTP)–bound form (fig. S2) (13). The sequence homology comparison of PM-localized small GTPases in Fig. 1C shows that closely homologous small GTPases can have different targeting

motifs. We also confirmed, for the examples of Rit and KRas, that polybasic targeting motifs alone can be sufficient for PM targeting (Fig. 1D).

To test whether polybasic clusters are anchored to the PM by binding to PI(4,5)P₂ (14), we hydrolyzed PM PI(4,5)P₂ by rapid targeting of Inp54p, a 5' specific PI(4,5)P₂ phosphatase (15), to the PM. This method is based on a PM-localized FK506-binding protein (FKBP12)–rapamycin-binding (FRB) construct and a cytosolic Inp54p enzyme conjugated with FKBP12 (CF-Inp) that can be translocated to the PM by chemical heterodimerization by using a rapamycin analog, iRap (16).

In experiments where we monitored PI(4,5)P₂ using a yellow fluorescent protein (YFP)–conjugated pleckstrin homology (PH) domain from phospholipase Cδ (PLCδ) (17), PM translocation of CF-Inp triggered a rapid and near complete dissociation of the YFP-PLCδ-PH domain from the PM (Fig. 2A). Despite this marked reduction in PI(4,5)P₂ concentration, only a small fraction of the polybasic-nonlipid tail fragment of Rit dissociated from the PM (Fig. 2B), which suggests that PI(4,5)P₂ is not alone responsible for PM targeting. Parallel experiments suggested that phosphatidylinositol 3,4,5-trisphosphate [PI(3,4,5)P₃] might be involved, because stimulation of cells with platelet-derived growth factor

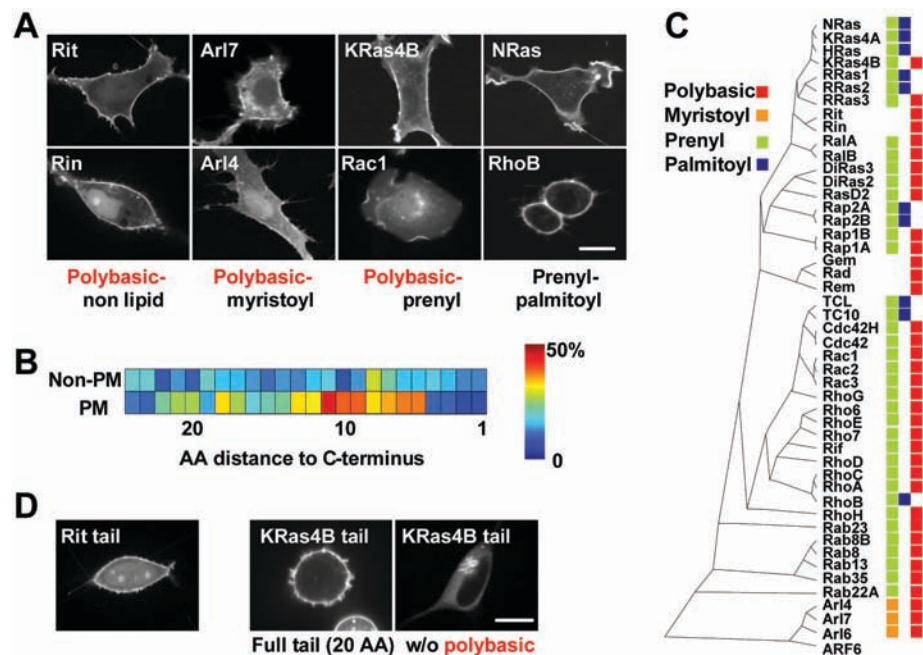


Fig. 1. A survey of the subcellular localization of 125 small GTPases shows that most PM-localized small GTPases have targeting motifs with clusters of polybasic amino acids. **(A)** Confocal images of the subcellular localization of CFP-conjugated small GTPases in NIH3T3 cells (full set of images in NIH3T3 and HeLa cells in fig. S1). The four main PM-targeting motifs are represented in the image panels. **(B)** Correlation between PM localization and the presence of lysine residues in a region 5 to 20 amino acids from the C terminus. **(C)** Phylogenetic tree of 48 small GTPases that were identified to be partially or fully localized to the PM. Individual membrane targeting elements are color coded: red for polybasic clusters and blue, green, and orange for palmitoyl, prenyl, and myristoyl consensus sequences, respectively. **(D)** Twenty-amino-acid-long C-terminal tail fragments of Rit and KRas are PM-localized. Lack of PM targeting of a KRas tail fragment without the polybasic region (right). Scale bars, 10 μ m.

¹Department of Molecular Pharmacology, 318 Campus Drive, Clark Building, Stanford University Medical School, Stanford, CA 94305, USA. ²Division of Applied Life Science (BK21 Program) and Environmental Biotechnology National Core Research Center, Gyeongsang National University, Jinju 660-701, Korea.

*To whom correspondence should be addressed. E-mail: tobias1@stanford.edu

(PDGF) led to a small increase in PM localization of the Rit tail and this small effect could be reversed by addition of an inhibitor of phosphoinositide 3-kinase (PI 3-kinase), LY294002

(LY29) (Fig. 2C; control experiments in fig. S3). Strikingly, the combined reduction of both PI(4,5)P₂ and PI(3,4,5)P₃ concentration triggered a dissociation of most Rit tail protein from

the PM (Fig. 2, D and E). The effect of reducing either PI(4,5)P₂ or PI(3,4,5)P₃ concentration alone on Rit tail localization was relatively small (Fig. 2E).

We also found that both PI(4,5)P₂ and PI(3,4,5)P₃ have to be lowered to significantly dissociate a tail fragment of Rin and a polybasic effector domain peptide from myristoylated alanine-rich C kinase substrate (MARCKS) protein (MARCKS ED) from the PM (Fig. 2, D and E). This MARCKS ED peptide was included because it has been extensively used for in vitro biochemical studies of the interaction between polybasic amino acids and phosphatidyserine and PI(4,5)P₂ (7, 14, 18, 19). HRas, which has a prenyl-palmitoyl PM-targeting motif without a polybasic cluster, did not dissociate from the PM after depletion of PI(4,5)P₂ and PI(3,4,5)P₃ (Fig. 2E). Control experiments with the same constructs in HeLa cells showed similar results (fig. S4), and an analysis of the dissociation kinetics showed that PM dissociation occurs within minutes after CF-Inp activation and LY29 addition (fig. S5A). We also verified that PM dissociation of polybasic proteins occurred when we combined PI(4,5)P₂ depletion with addition of wortmannin, an alternative PI 3-kinase inhibitor, or with expression of a dominant negative PI 3-kinase inhibitory construct (20) (figs. S6 and S7). Additional control experiments are shown in figs. S8 to S12, including in vitro lipid-blot assays that showed enhanced affinity of proteins with polybasic clusters for PI(3,4,5)P₃ over PI(4,5)P₂. These control experiments strengthen the argument that PI(4,5)P₂ and the less abundant PI(3,4,5)P₃ both serve as PM anchors for proteins with polybasic clusters.

Insights into the electrostatic binding mechanism between positively charged polybasic clusters and negatively charged polyphosphoinositides came from a sequence comparison of nonprenylated PM-targeted small GTPases. Most of these proteins contain two or three subclusters of polybasic residues in the C-terminal tail. Each subcluster spans about four or five amino acids, and the mean distance between subclusters is nine amino acids (Fig. 3A). Consistent with a need for multiple subclusters, the removal of a flanking subcluster in the Rit tail was sufficient to abolish PM targeting (Rit tail 199 to 219) (Fig. 3B). This suggests that PM targeting results from additive binding energy of individual subclusters that each electrostatically interact with a PI(4,5)P₂ or PI(3,4,5)P₃ lipid. Selectivity for polyphosphoinositides over phosphatidyserine may occur because of opposing high relative-charge densities of polyphosphoinositides and polybasic subclusters (7).

We then investigated differences between the targeting mechanisms of the three polybasic-nonlipid, polybasic-myristoyl, and polybasic-prenyl PM-targeting motifs. A distinct feature of the polybasic-nonlipid targeting motifs is their similarity to nuclear localization sequences. We found hydrophobic amino acids to be im-

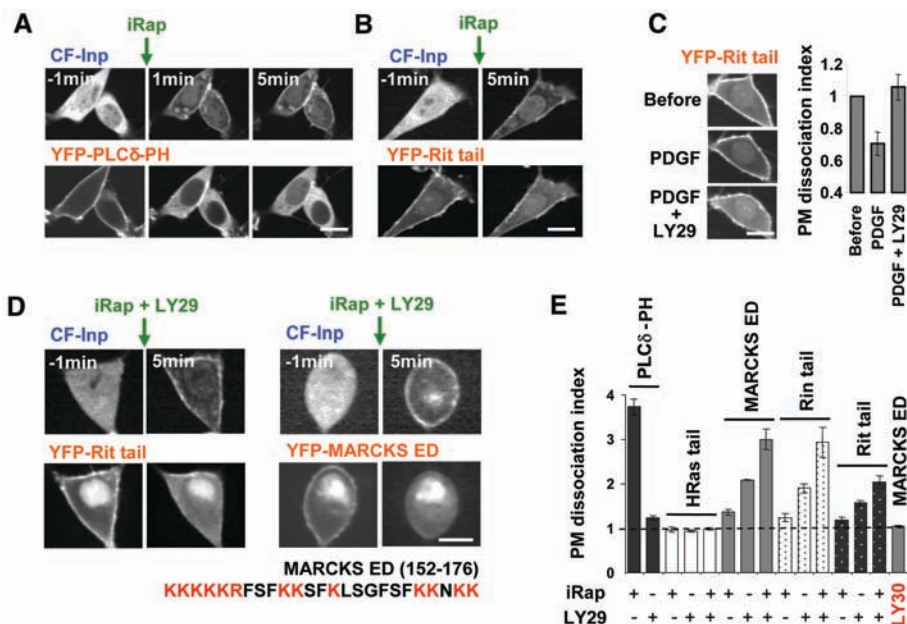


Fig. 2. Depletion of PI(4,5)P₂ and PI(3,4,5)P₃ dissociates Rit, Rin, and MARCKS ED with polybasic-nonlipid targeting motifs from the PM. (A) Development of a chemically inducible translocation method to deplete PI(4,5)P₂ from the inner leaflet of the PM (22, 23). The PI(4,5)P₂ biosensor YFP-PLCδ-PH was cotransfected to monitor depletion of PI(4,5)P₂. (B) Depletion of PI(4,5)P₂ caused only a small reduction in the PM localization of YFP-conjugated Rit tail. (C) A small, but significant, PDGF receptor-mediated increase in Rit tail PM localization can be reversed by addition of the PI3-kinase inhibitor LY29 (before and 9 min after addition of 5 μM iRap). The bar graph shows a quantification of the same experiment. The PM dissociation index is the relative ratio of internal over PM fluorescence; that is, $F_{1cyt}/F_{1PM} * F_{0PM}/F_{0cyt}$, with F_0 and F_1 as the fluorescent intensities before and after PI(4,5)P₂ and PI(3,4,5)P₃ depletion. (D) Joint reduction in PI(4,5)P₂ and PI(3,4,5)P₃ triggered a near-complete dissociation of Rit tail and MARCKS ED from the PM. (E) Quantitative analysis of the CF-Inp and/or LY29-triggered PM dissociation of MARCKS ED, and Rit and Rin tails. PLCδ-PH and HRas tails are shown as controls. The inactive LY29 analog LY30 was used as a control (24). Scale bars, 10 μm.

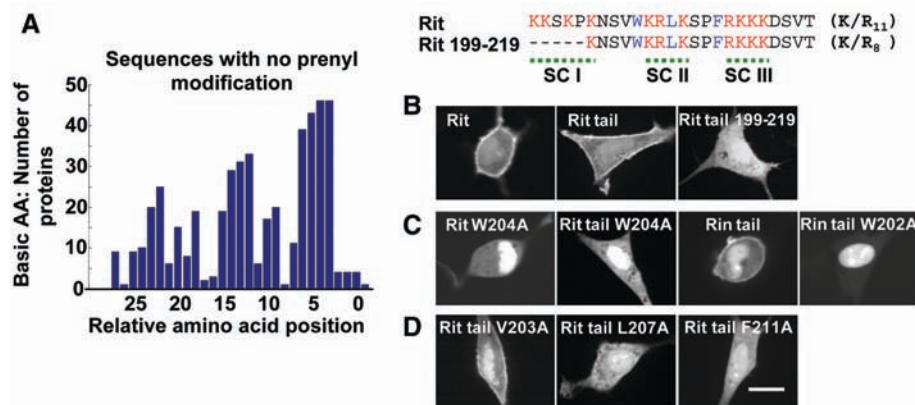
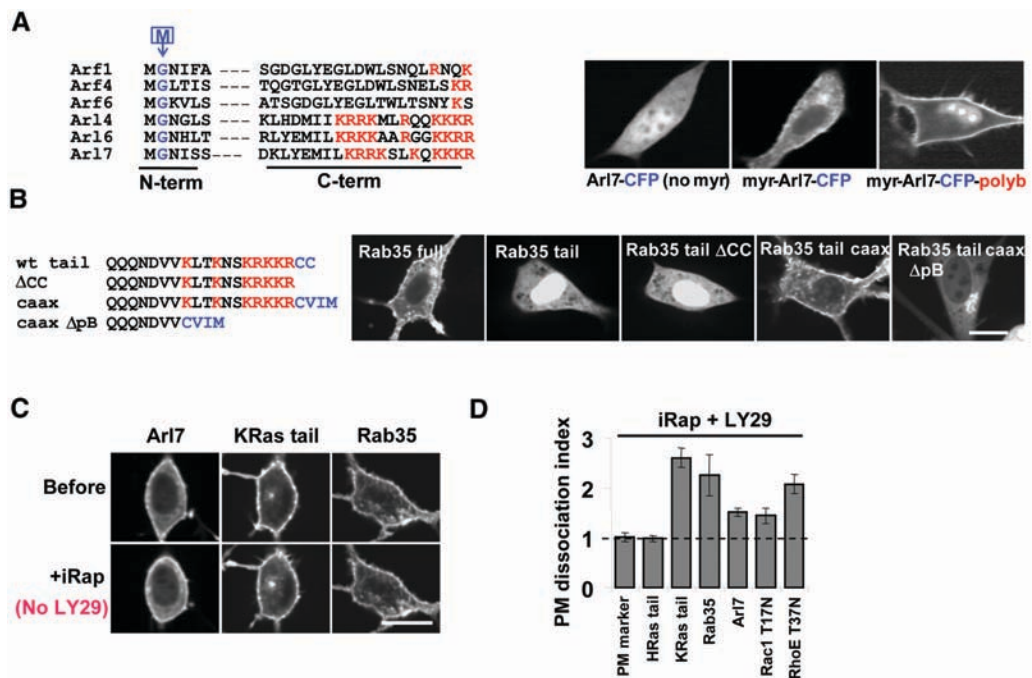


Fig. 3. Polybasic subclusters and hydrophobic amino acids are required for PM targeting by polybasic-nonlipid targeting motifs. (A) Statistical analysis of the relative sequence location of positively charged amino acids in nonprenylated small GTPases. (B) Loss of PM targeting of Rit tail fragment after removal of a single subcluster with positively charged amino acids. (C) Identification of a tryptophan residue in the polybasic regions of Rit and Rin that mediates PM over nuclear localization. Full-length small GTPases, as well as tail fragment mutants, are shown. (D) Identification of two additional hydrophobic amino acid residues that contribute to the PM targeting of Rit. Scale bars, 10 μm.

Fig. 4. Depletion of PI(4,5)P₂ and PI(3,4,5)P₃ dissociates proteins with polybasic-myristoyl and polybasic-prenyl targeting motifs from the PM. **(A)** Aligned sequences of the N terminus (6 amino acids) and C terminus (20 amino acids) of six ARF family members. Confocal images of an Arl7 mutant construct lacking the N-terminal myristoylation motif (left), a C-terminal tagged Arl7 control construct (middle), and a mutant construct with an internal CFP tag and a flexible C-terminal polybasic Arl7 tail (right). **(B)** PM localization motifs in geranylgeranylated Rab35. Confocal images from left to right: localization of wild-type Rab35, wild-type tail fragment, wild-type tail lacking geranylgeranylation motif (Δ CC), Rab35 tail Δ CC mutant with KRas caax (Rab35 tail caax), and Rab35 tail caax mutant lacking polybasic amino acids (Rab35 tail caax Δ pB). **(C)** Depletion of PI(4,5)P₂ by CF-Inp activation without L29 addition causes only a minimal PM dissociation of Arl7, KRas tail fragment, and Rab35. **(D)** Quantitative analysis of the much larger PM dissociation of polybasic-lipid modified proteins after depletion of PI(4,5)P₂ and PI(3,4,5)P₃ by CF-Inp activation and addition of LY29. Scale bars, 10 μ m.



portant for selective PM localization, because site-directed mutagenesis of a single hydrophobic amino acid (Trp²⁰⁴Ala in Rit or Trp²⁰²Ala in Rin) led to a complete loss of PM targeting and a strong nuclear localization (Fig. 3C). A loss of PM targeting but with less nuclear targeting could also be observed for Leu²⁰⁷Ala and Phe²¹¹Ala Rit mutants (Fig. 3D) and for hydrophobic amino acid mutants of the small GTPases GEM and RAD (fig. S13). Thus, hydrophobic amino acids strengthen PM binding of polybasic-nonlipid motifs and prevent the polybasic cluster from functioning as a nuclear localization sequence.

The polybasic-myristoyl PM-targeting motifs have the distinct feature of a separated N-terminal myristoylation consensus sequence and a C-terminal polybasic cluster. Mutant constructs showed that effective PM targeting of Arl7 required an N-terminal myristoyl motif (left panel, Fig. 4A), as well as a flexible C-terminal polybasic tail (middle versus right panel, Fig. 4A), which suggests that the two ends of the protein synergistically support PM targeting.

The polybasic-prenyl PM-targeting motif includes proteins such as KRas for which a 20-amino acid tail sequence is sufficient for farnesylation and PM targeting (Fig. 1D), as well as Rab35 for which an intact GTPase domain is required for geranylgeranylation (27) and for PM targeting (second and third panels, Fig. 4B). We further compared the roles of farnesylation and geranylgeranylation by creating a Rab35 mutant with a consensus CAAX farnesylation sequence in place of the geranylgeranylation sequence. This mutant showed PM localization indistinguishable from that of the geranylgeranylated

Rab35 (fourth panel, Fig. 4B). We also confirmed that the PM targeting of RAB35 requires a polybasic cluster (last panel, Fig. 4B). This shows that the polybasic-geranylgeranyl motifs of Rab35 can be equally effective in PM targeting as the polybasic-farnesyl motif of KRas, which supports the notion that both types of prenylation motifs can be grouped into a single polybasic-prenyl PM-targeting motif.

We then tested whether PI(4,5)P₂ and PI(3,4,5)P₃ also regulate polybasic-myristoyl and polybasic-prenyl targeting motifs. As for the polybasic-nonlipid targeting motif, depletion of PI(4,5)P₂ alone triggered only a minor reduction in PM localization of the Arl7 polybasic-myristoyl targeting motif and the KRas and Rab35 polybasic-prenyl motifs (Fig. 4C). Depletion of both PI(4,5)P₂ and PI(3,4,5)P₃ triggered significant PM dissociation of all polybasic-myristoyl and polybasic-prenyl constructs tested (Fig. 4D) with a kinetics similar to that of Rit (fig. S5), which suggests that PI(4,5)P₂ and PI(3,4,5)P₃ have the same role for PM localization for all three types of polybasic PM-targeting motifs. HRas was again included as a control protein without a polybasic cluster.

Our study shows that polybasic PM-targeting motifs are built from two parts, an unspecific membrane-targeting part that can be hydrophobic amino acids, myristoyl groups, or prenyl groups and a polybasic targeting part that provides PM specificity by binding of positively charged amino acid clusters to negatively charged PI(4,5)P₂ and PI(3,4,5)P₃ lipids in the PM. This gives PI(4,5)P₂ and PI(3,4,5)P₃ a ubiquitous role in regulating signaling, cytoskeletal, and transport proteins and argues that

these lipid second messengers function as signaling hubs in cellular control systems.

References and Notes

1. M. Fivaz, T. Meyer, *Neuron* **40**, 319 (2003).
2. M. N. Teruel, T. Meyer, *Cell* **103**, 181 (2000).
3. J. L. Guan, *Science* **303**, 773 (2004).
4. D. Michaelson et al., *J. Cell Biol.* **152**, 111 (2001).
5. K. A. Cadwallader, H. Paterson, S. G. Macdonald, J. F. Hancock, *Mol. Cell Biol.* **14**, 4722 (1994).
6. F. Ghomashchi, X. Zhang, L. Liu, M. H. Gelb, *Biochemistry* **34**, 11910 (1995).
7. S. McLaughlin, D. Murray, *Nature* **438**, 605 (2005).
8. W. D. Heo, T. Meyer, *Cell* **113**, 315 (2003).
9. A. Schurmann et al., *J. Biol. Chem.* **269**, 15683 (1994).
10. E. Choy et al., *Cell* **98**, 69 (1999).
11. C. H. Lee, N. G. Della, C. E. Chew, D. J. Zack, *J. Neurosci.* **16**, 6784 (1996).
12. O. Rocks et al., *Science* **307**, 1746 (2005).
13. H. Radhakrishna, J. G. Donaldson, *J. Cell Biol.* **139**, 49 (1997).
14. S. McLaughlin, J. Wang, A. Gambhir, D. Murray, *Annu. Rev. Biophys. Biomol. Struct.* **31**, 151 (2002).
15. T. Inoue, W. D. Heo, J. S. Grimley, T. J. Wandless, T. Meyer, *Nat. Methods* **2**, 415 (2005).
16. D. Raucher et al., *Cell* **100**, 221 (2000).
17. T. P. Stauffer, S. Ahn, T. Meyer, *Curr. Biol.* **8**, 343 (1998).
18. J. Wang, A. Arbutova, G. Hangyas-Mihalayne, S. McLaughlin, *J. Biol. Chem.* **276**, 5012 (2001).
19. C. Chapline, K. Ramsay, T. Klauk, S. Jaken, *J. Biol. Chem.* **268**, 6858 (1993).
20. S. Poser, S. Impey, K. Trinh, Z. Xia, D. R. Storm, *EMBO J.* **19**, 4955 (2000).
21. M. C. Seabra, C. Wasmeier, *Curr. Opin. Cell Biol.* **16**, 451 (2004).
22. B.-C. Suh, T. Inoue, T. Meyer, B. Hille, *Science* **314**, 1454 (2006); published online 21 September 2006; 10.1126/science.1131163.
23. Correspondence about the iRap inducible enzyme systems should be directed to T. Inoue (e-mail: jctinoue@stanford.edu).
24. T. W. Poh, S. Pervaiz, *Cancer Res.* **65**, 6264 (2005).
25. We thank A. Salmeen, M. F. Teruel, M. Fivaz, and other members of the Meyer laboratory for support; A. R. Koh and S. H. Ryu (POSTECH) for critical reading of the

manuscript; S. McLaughlin (SUNY Stony Brook) and B. Hille (U. Washington) for discussions; and James Whalen for assisting with the in vitro lipid-binding assays. T.I. is a recipient of a fellowship from the Quantitative Chemical Biology Program. B.O.P. was supported by a grant from KOSEF/MOST EB-NCRC (grant no. R15-2003-012-01001-0) and by scholarships from the Brain Korea 21 program.

This work was supported by grants from National Institute of Mental Health and National Institute of General Medical Sciences, NIH, to T.M.

Supporting Online Material
www.sciencemag.org/cgi/content/full/1134389/DC1
Materials and Methods

Figs. S1 to S13
References

28 August 2006; accepted 11 October 2006
Published online 9 November 2006;
10.1126/science.1134389
Include this information when citing this paper.

A Genome-Wide Association Study Identifies *IL23R* as an Inflammatory Bowel Disease Gene

Richard H. Duerr,^{1,2} Kent D. Taylor,^{3,4} Steven R. Brant,^{5,6} John D. Rioux,^{7,8} Mark S. Silverberg,⁹ Mark J. Daly,^{8,10} A. Hillary Steinhart,⁹ Clara Abraham,¹¹ Miguel Regueiro,¹ Anne Griffiths,¹² Themistocles Dassopoulos,⁵ Alain Bitton,¹³ Huiying Yang,^{3,4} Stephan Targan,^{4,14} Lisa Wu Datta,⁵ Emily O. Kistner,¹⁵ L. Philip Schumm,¹⁵ Annette T. Lee,¹⁶ Peter K. Gregersen,¹⁶ M. Michael Barmada,² Jerome I. Rotter,^{3,4} Dan L. Nicolae,^{11,17} Judy H. Cho^{18*}

The inflammatory bowel diseases Crohn's disease and ulcerative colitis are common, chronic disorders that cause abdominal pain, diarrhea, and gastrointestinal bleeding. To identify genetic factors that might contribute to these disorders, we performed a genome-wide association study. We found a highly significant association between Crohn's disease and the *IL23R* gene on chromosome 1p31, which encodes a subunit of the receptor for the proinflammatory cytokine interleukin-23. An uncommon coding variant (rs11209026, c.1142G>A, p.Arg381Gln) confers strong protection against Crohn's disease, and additional noncoding *IL23R* variants are independently associated. Replication studies confirmed *IL23R* associations in independent cohorts of patients with Crohn's disease or ulcerative colitis. These results and previous studies on the proinflammatory role of IL-23 prioritize this signaling pathway as a therapeutic target in inflammatory bowel disease.

Crohn's disease (CD) and ulcerative colitis (UC), the two common forms of idiopathic inflammatory bowel disease (IBD), are chronic, relapsing inflammatory disorders of the gastrointestinal tract. Each has a peak age of onset in the second to fourth decades of life and prevalences in European ancestry populations that average about 100 to 150 per 100,000 (1, 2). Although the precise etiology of IBD remains to be elucidated, a widely accepted hypothesis is that ubiquitous, commensal intestinal bacteria trigger an inappropriate, overactive, and ongoing mucosal immune response that mediates intestinal tissue damage in genetically susceptible individuals (1). Genetic factors play an important role in IBD pathogenesis, as evidenced by the increased rates of IBD in Ashkenazi Jews, familial aggregation of IBD, and increased concordance for IBD in monozygotic compared to dizygotic twin pairs (3). Moreover, genetic analyses have linked IBD to specific genetic variants, especially *CARD15* variants on chromosome 16q12 and the *IBD5* haplotype (spanning the organic cation transporters, *SLC22A4* and *SLC22A5*, and other genes) on chromosome 5q31 (3–7). CD and UC are thought to be related disorders that share some genetic susceptibility loci but differ at others.

The replicated associations between CD and variants in *CARD15* and the *IBD5* haplotype do not fully explain the genetic risk for

CD, so we performed a genome-wide association study testing 308,332 autosomal single nucleotide polymorphisms (SNPs) on the Illumina HumanHap300 Genotyping BeadChip (8). Our study population consisted of 567 non-Jewish, European ancestry patients with ileal CD and 571 non-Jewish controls. We initially focused on ileal CD, the most common location of CD, to minimize pathogenic heterogeneity. After exclusion of study subjects with genotype completion rates less than 94%, we included 547 cases and 548 controls in subsequent analyses (8). Single-marker allelic tests were performed using χ^2 statistics for all autosomal markers. Three SNPs had nearly two orders of magnitude greater significance compared to the next most significant markers, and they are the only markers that remain significant at the 0.05 level after Bonferroni correction. Two of the three markers, rs2066843 ($P = 2.86 \times 10^{-9}$, corrected $P = 8.82 \times 10^{-4}$) and rs2076756 ($P = 5.12 \times 10^{-10}$, corrected $P = 1.58 \times 10^{-4}$), are in the known CD susceptibility gene, *CARD15* (4, 5). The third marker, rs11209026 ($P = 5.05 \times 10^{-9}$, corrected $P = 1.56 \times 10^{-3}$), is a nonsynonymous SNP (c.1142G>A, p.Arg381Gln) in the *IL23R* gene (GenBank accession: NM_144701, GeneID: 149233) on chromosome 1p31. This gene encodes a subunit of the receptor for the proinflammatory cytokine, interleukin-23 (IL-23), and is therefore an intriguing functional can-

didate. In addition to Arg381Gln, nine other markers in *IL23R* and in the intergenic region between *IL23R* and the adjacent IL-12 receptor, beta-2 gene (*IL12RB2*), had association P -values < 0.0001 in the non-Jewish, ileal CD case-control cohort (Table 1 and table S1a).

We next tested for association of *IL23R* markers in an independent ileal CD case-control cohort, consisting of 401 patients and 433 controls, all of Jewish ancestry (8). Significant associations were observed for several of the same markers that were associated in the non-Jewish cohort (Table 1 and table S1b). In a combined analysis of the data from the two ileal CD case-control cohorts (8), nine markers had highly significant association P -values ranging from 1.60×10^{-9} to 3.36×10^{-13} (Table 1 and table S1b).

We then extended the replication study by performing family-based association testing of 27 *IL23R* region markers in an independent cohort of 883 nuclear families in which both par-

¹Division of Gastroenterology, Hepatology and Nutrition, Department of Medicine, School of Medicine, University of Pittsburgh, University of Pittsburgh Medical Center Presbyterian, Mezzanine Level, C-Wing, 200 Lothrop Street, Pittsburgh, PA 15213, USA. ²Department of Human Genetics, Graduate School of Public Health, University of Pittsburgh, Crabtree A300, 130 Desoto Street, Pittsburgh, PA 15261, USA. ³Medical Genetics Institute, Cedars-Sinai Medical Center, 8700 Beverly Boulevard, Los Angeles, CA 90048, USA. ⁴IBD Center, Division of Gastroenterology, Cedars-Sinai Medical Center, 8700 Beverly Boulevard, Los Angeles, CA 90048, USA. ⁵Harvey M. and Lyn P. Meyerhoff Inflammatory Bowel Disease Center, Department of Medicine, Johns Hopkins University School of Medicine, B136, 1503 East Jefferson Street, Baltimore, MD 21231, USA. ⁶Department of Epidemiology, Bloomberg School of Public Health, Johns Hopkins University, 615 North Wolfe Street, Baltimore, MD 21205, USA. ⁷Université de Montréal and the Montreal Heart Institute, 5-6400, 5000 Belanger Street, Montreal, Quebec H1T 1C8, Canada. ⁸Medical and Population Genetics Program, Broad Institute of MIT and Harvard, 7 Cambridge Center, Cambridge, MA 02142, USA. ⁹Mount Sinai Hospital IBD Centre, University of Toronto, 441-600 University Avenue, Toronto, Ontario M5G 1X5, Canada. ¹⁰Massachusetts General Hospital, Harvard Medical School, 185 Cambridge Street, Boston, MA 02114, USA. ¹¹Department of Medicine, University of Chicago, 5841 South Maryland Avenue, Chicago, IL 60637, USA. ¹²Department of Pediatrics, The Hospital for Sick Children, 555 University Avenue, Toronto, Ontario M5G 1X8, Canada. ¹³Royal Victoria Hospital, McGill University Health Centre, 687 Pine Avenue West, Montreal, Quebec H3A 1A1, Canada. ¹⁴Immunobiology Research Institute, Cedars-Sinai Medical Center, Davis 4063, 8700 Beverly Boulevard, Los Angeles, CA 90048, USA. ¹⁵Department of Health Studies, University of Chicago, 5841 South Maryland Avenue, Chicago, IL 60637, USA. ¹⁶The Feinstein Institute for Medical Research, 350 Community Drive, Manhasset, NY 11030, USA. ¹⁷Department of Statistics, University of Chicago, 5734 South University Avenue, Chicago, IL 60637, USA. ¹⁸IBD Center, Section of Digestive Diseases, Departments of Medicine and Genetics, Yale University, S155A, 300 Cedar Street, New Haven, CT 06519, USA.

*To whom correspondence should be addressed. E-mail: judy.cho@yale.edu